Characterizing a defect in a one-dimensional bar

Cynthia Gangi, and Sameer Shah

January 21, 2003

Abstract

We examine the inverse problem of locating and describing an internal point defect in a one-dimensional rod Ω by controlling the heat inputs and measuring the subsequent temperatures at the boundary of Ω. We use a variation of the forward heat equation to model heat flow through Ω, then propose algorithms for locating an internal defect and quantifying the effect the defect has on the heat flow. We implement these algorithms, analyze the stability of the procedures, and provide several computational examples.

Contents

1 Introduction

In this paper we study the noninvasive use of thermal energy to detect the presence of a defect in the interior of an object. Specifically, consider a one-dimensional rod Ω which contains a point "defect" in its interior. It is logical to assume that this defect will interfere with the heat flow in Ω. We model the defect as a point "contact resistance," quantified below. One method to determine the defect's location and the nature of its impact on the heat flow is to input a heat flux at both ends of Ω and record the subsequent temperature measurements at these ends for a certain length of time. The presence of a defect, since it alters the heat flow, will manifest itself in the resulting temperature behavior at the endpoints. The goal of this research is to determine if this method of thermal imaging can indeed be employed to successfully find the location and nature of the defect.

This investigation is an extension of the work done by Bryan and Caudill ([1]) on the well-posedness of the forward problem for heat flow in a bar with a point defect under reasonable boundary conditions. The authors demonstrate the existence and uniqueness of classical solutions to this problem. Our research addresses the inverse version of the same problem, in which the goal is to identify internal characteristics (the defect) from boundary data.

The application of inverse problem-solving arises in an area known as *non-destructive testing*, which uses thermal imaging on the surface of an object to locate an internal defect. In other words, by only having knowledge of the boundary of an object, internal blemishes can be characterized without the object's destruction. In our case, it will be shown that merely controlling the boundary heat fluxes of Ω and measuring the resulting boundary temperatures, recovery of the location and nature of a defect is possible.

The inverse problem will be considered in two separate versions– continuous data and finite data. The continuous data version assumes temperature measurements at the endpoints are known for all time while the finite data version assumes that temperature measurements are known for only a finite time interval.

In section 2 we present a mathematical model for the flow of heat through a one-dimensional rod with an interior defect will be presented. The model is an initial-boundary value problem for the heat equation with a component that describes the defect. The defect is modelled as an internal point whose heat flux is governed by the temperature jump at its site rather than the otherwise-applicable heat equation.

The justification for utilizing a zero initial temperature distribution is presented in section 3. In section 4, we establish that the location of the defect is uniquely determined by the endpoint temperature measurements and show the recovery of the function defining the defect. Sections 5, 6, and 7 address the finite data version of the recovery of the location of the defect and the function describing it. We discuss the concept of ill-posedness and how to mitigate this phenomenon, along with providing examples of reconstructions, in section 8. Lastly we present a conclusion in section 9.

2 The Forward Problem

Consider a one-dimensional rod Ω on the interval $(0, 1)$. We use x for spatial position, t for time, and $u(t, x)$ for the temperature of the bar at position x and time t. After re-scaling we may assume both thermal diffusivity and conductivity are equal to one. We assume the interior of the object contains a defect at $x = \sigma$, $0 < \sigma < 1$, which impedes the flow of heat in the rod, as quantified below.

We assume that the defect causes a jump in the temperature at its site since we model the defect as a resistance to heat flow between the regions on both sides of it. The nature of the defect's impedance of the heat flow will be based solely on this temperature jump. In addition, we assume the heat flux, given as $u_x(t, x)$, is continuous across $x = \sigma$ so that the point σ does not store energy. Let $u(t, x)$ be the temperature in the bar, and define $[u](t) = \lim_{x\to\sigma^+} u(t, x) - \lim_{x\to\sigma^-} u(t, x)$ to

be the temperature jump at $x = \sigma$. We model the defect as $u_x(t, \sigma) = F([u](t))$, where F is a non-decreasing, Lipschitz continuous function with $F(0) = 0$. The function F governs how the heat flux and temperature jump over the defect are related, with $F \equiv 0$ modelling a perfectly insulating defect.

We thus assume that $u(t, x)$ satisfies the initial-boundary value problem

$$\begin{aligned} u_t(t,x) - u_{xx}(t,x) &= 0 \text{ for } x \in (0,\sigma) \cup (\sigma, 1),\ t > 0 && (1)\\ -u_x(t,0) &= g_0(t) && (2)\\ u_x(t,1) &= g_1(t) && (3)\\ u_x(t,\sigma) &= F([u](t)) && (4)\\ u(0,x) &= f(x) && (5) \end{aligned}$$

in which $f(x)$ denotes the initial temperature of the region and $g_0(t), g_1(t)$ the input heat fluxes at $x = 0$ and $x = 1$, respectively. It was proved in [1] that this forward problem is well-posed, and there exists a unique solution which is in $C^1[0, \sigma]$ and $C^1[\sigma, 1]$ for all $t > 0$.

Some simplifying assumptions can be made. In general, we will assume that the initial condition is $f(x) = 0$. This will be explained in section 3. Also, we will generally assume that $g_0(t)$ and $g_1(t)$ are piecewise continuous and supported for $t \leq R$ for some positive constant R.

As mentioned above, take F to be non-decreasing with $F(0) = 0$. The reasoning for this is as follows: Heat flows in proportion to the temperature gradient, from a region of higher temperature to a region of lower temperature. Since F describes the heat flow across the defect in terms of the temperature jump, when the temperature difference at the defect is positive (the temperature to the immediate right of the defect is greater than the temperature to its immediate left), the heat flow will also be positive. We expect that the greater the jump is at the defect, the greater the heat flow will be through it. Thus F is non-decreasing (and in practice, strictly increasing). Furthermore, if there is no temperature difference at the defect, heat will not flow through it, and thus $F(0) = 0$.

In addition, the following assumptions are made:

A1. The input fluxes g_0 and g_1 are not both identically zero, and the total input energy is finite, so $\int_0^\infty g_0(t)dt < \infty$ and $\int_0^\infty g_1(t)dt < \infty$.

A2. F is uniformly Lipschitz continuous on any bounded interval, i.e. for any $a > 0$ we have $|F(x) - F(y)| \leq C(a)|x - y|$ for some constant $C(a)$.

A3. $F(x)$ acts linearly near $x = 0$, so $xF(x) \geq kx^2$ for some constant $k > 0$.

3 Preliminaries

In this section we note two results that will be useful in the following sections.

Theorem 3.1 *Let $u_1(t, x)$ and $u_2(t, x)$ be solutions to the heat equation for $t_1 < t < t_2$ and $0 < x < c$, continuously differentiable for $x \in [0, c]$, with $u_1(t, 0) \equiv u_2(t, 0)$ and $\frac{\partial u_1}{\partial x}(t, 0) \equiv \frac{\partial u_2}{\partial x}(t, 0)$ for $t_1 < t < t_2$. Then $u_1(t, x) \equiv u_2(t, x)$ for $t_1 < t < t_2$ and $0 < x < c$.*

This is a direct consequence of Theorem 11.4.1 in [2].

Throughout the rest of the paper we will, for simplicity, take the initial condition for Ω as $f(x) = 0$. The validity of this can be ascertained by showing that after a long period of time, the solution to the boundary value problem (1)-(5) will decay to a constant, as quantified by Theorem 3.2 below. This temperature can then be re-scaled to zero, thus giving zero initial conditions to the bar. This result will also be useful for later error analysis.

Theorem 3.2 *Let $u(t, x)$ satisfy the heat equation on $(0, \sigma) \cup (\sigma, 1)$ with zero flux boundary conditions at $x = 0$ and $x = 1$, $u(0, x) = f(x)$ and jump condition $u_x(t, \sigma) = F([u](t))$, where F satisfies the*

assumptions specified in the previous section. Then,

$$\int_0^1 (u(t,x)-c)^2 dx \le Ce^{-2kt/(4k+1)}$$

for some constants $C, c,$ and $k > 0$.

Proof. Let $c = \int_0^1 f(x)dx$ and $v(t,x) = u(t,x) - c$, so $v(t,x)$ satisfies the heat equation on $(0,\sigma) \cup (\sigma,1)$ with zero flux boundary conditions at $x = 0$ and $x = 1$, $v(0,x) = f(x) - c$, and jump condition $v_x(t,\sigma) = F([v](t))$.

We can compute, using integration by parts, the fact that v satisfies the heat equation, and the zero flux boundary conditions, that

$$\begin{aligned}
\frac{\partial}{\partial t}(\frac{1}{2}\int_0^\sigma v^2(t,x)dx) &= v^-(t,\sigma)v_x(t,\sigma) - \int_0^\sigma v_x^2(t,y)dy \\
\frac{\partial}{\partial t}(\frac{1}{2}\int_\sigma^1 v^2(t,x)dx) &= -v^+(t,\sigma)v_x(t,\sigma) - \int_\sigma^1 v_x^2(t,y)dy
\end{aligned}$$

Adding these two equations yields

$$\frac{\partial}{\partial t}(\frac{1}{2}\int_0^1 v^2(t,x)dx) = -F([v](t))[v](t) - \int_0^1 v_x^2(t,y)dy. \tag{6}$$

To find a bound for $v(t,x)$ itself, let x_0 be a point in $(0,\sigma)$. We find for any $x \in (0,\sigma)$

$$\begin{aligned}
|v(t,x)| &= |\int_{x_0}^x v_x(t,y)dy + v(t,x_0)| \\
&\le \sqrt{|x-x_0|}(\int_0^\sigma v_x^2(t,y)dy)^{1/2} + |v(t,x_0)| \\
&\le (\int_0^1 v_x^2(t,y)dy)^{1/2} + |v(t,x_0)| \qquad (7)
\end{aligned}$$

where we have used Hölder's inequality, $\int fg \le (\int f^2)^{1/2}(\int g^2)^{1/2}$, with $g \equiv 1$. If $x \in (\sigma,1)$ (but still the same $x_0 \in (0,\sigma)$) we find that

$$\begin{aligned}
|v(t,x)| &= |v^-(t,\sigma) + [v](t) + \int_\sigma^x v_x(t,y)dy| \\
&\le (\int_0^1 v_x^2(t,y)dy)^{1/2} + |v(t,x_0)| + |[v](t)| + \sqrt{|x-\sigma|}(\int_\sigma^x v_x^2(t,y)dy)^{1/2} \\
&\le (\int_0^1 v_x^2(t,y)dy)^{1/2} + |v(t,x_0)| + |[v](t)| + (\int_0^1 v_x^2(t,y)dy)^{1/2} \\
&= 2(\int_0^1 v_x^2(t,y)dy)^{1/2} + |v(t,x_0)| + |[v](t)| \qquad (8)
\end{aligned}$$

We now choose our x_0. We know $\int_0^1 v(t,x)dx = 0$ for all t from the following (which uses the facts that v satisfies the heat equation and that there are zero input fluxes at $x = 0$ and $x = 1$):

$$\frac{\partial}{\partial t}(\int_0^1 v(t,x)dx) = \int_0^1 v_t(t,x)dx = \int_0^1 v_{xx}(t,x)dx = 0.$$

This implies either there exists an x_0 such that $v(t,x_0) = 0$, or if no such x_0 exists, that $v(t,x) < 0$ for $x < \sigma$ and $v(t,x) > 0$ (or vice-versa).

If there exists some $x_0 \in (0,\sigma)$ such that $v(t,x_0) = 0$ (for some fixed time t) then from (7) and/or (8),

$$|v(t,x)| \leq 2(\int_0^1 v_x^2(t,y)dy)^{1/2} + |[v](t)| \tag{9}$$

for all $x \in (0,1)$. A similar argument shows that (8) holds if there is some point x_0 in $(\sigma,1)$ with $v(t,x_0) = 0$.

However, if there is no point $x_0 \in (0,\sigma)$ or in $(\sigma,1)$ such that $v(t,x_0) = 0$ then this means that $v(t,x) < 0$ for $0 \leq x \leq \sigma$ and $v(t,x) > 0$ for $\sigma \leq x \leq 1$, or vice-versa. In this case, we can still establish inequality (9), for if without loss of generalization $v(t,x) < 0$ for $0 \leq x \leq \sigma$, then for $x \in (0,\sigma)$ we have

$$\begin{aligned} |v(t,x)| &= |\int_x^\sigma v_x(t,y)dy + v^-(t,\sigma)| \\ &\leq \sqrt{|\sigma - x|}\int_0^1 v_x^2(t,y)dy + |[v(t)]| \\ &\leq (\int_0^1 v_x^2(t,y)dy)^{1/2} + |[v](t)| \\ &\leq 2(\int_0^1 v_x^2(t,y)dy)^{1/2} + |[v](t)| \end{aligned}$$

since $|v^-(t,\sigma)| < |[v](t)|$ from the given assumptions. A similar argument holds for $x \in (\sigma,1)$. Therefore, inequality (9) is valid for all $x \in (0,1)$ at all times t.

Squaring both sides of (9) yields

$$v^2(t,x) \leq 4\int_0^1 v_x^2(t,x)dx + 4[v](t)(\int_0^1 v_x^2(t,y)dy)^{1/2} + ([v](t))^2. \tag{10}$$

From Young's inequality ($pq \leq \frac{p^2}{2\epsilon^2} + \frac{\epsilon^2 q^2}{2}$ for all ϵ) we have

$$[v(t)](\int_0^1 v_x^2(t,y)dy)^{1/2} \leq \frac{1}{2\epsilon^2}([v](t))^2 + \frac{\epsilon^2}{2}\int_0^1 v_x^2(t,y)dy$$

for any ϵ. Inserting this into (10) we obtain

$$v^2(t,x) \leq (4 + 2\epsilon^2)\int_0^1 v_x^2(t,y)dy - (1 + 2/\epsilon^2)([v](t))^2$$

and so (after integrating both sides from $x = 0$ to $x = 1$ and noting that the right side is constant in terms of x)

$$\int_0^1 v^2(t,x)dx \leq (4 + 2\epsilon^2)\int_0^1 v_x^2(t,y)dy + (1 + 2/\epsilon^2)([v](t))^2$$

or with a bit of rearrangement,

$$0 \leq \int_0^1 v_x^2(t,y)dy + \frac{1 + 2/\epsilon^2}{4 + 2\epsilon^2}([v](t))^2 - \frac{1}{4 + 2\epsilon^2}\int_0^1 v^2(t,x)dx. \tag{11}$$

Equation (11) can be combined with equation (6) to obtain

$$\frac{\partial}{\partial t}(\frac{1}{2}\int_0^1 v^2(t,x)dx) \leq -F([v](t))[v](t) + \frac{1 + 2/\epsilon^2}{4 + 2\epsilon^2}([v](t))^2 - \frac{1}{4 + 2\epsilon^2}\int_0^1 v^2(t,x)dx. \tag{12}$$

To conclude the proof of Theorem 3.2 we need

Lemma 3.1 *There exists an ϵ such that*

$$-yF(y) + \frac{1 + 2/\epsilon^2}{4 + 2\epsilon^2} y^2 \leq 0$$

for all y.

Proof. Recall that one restriction on F is $-yF(y) + ky^2 \leq 0$. Thus, it is necessary to show that an ϵ exists such that the equation

$$-ky^2 + \frac{1 + 2/\epsilon^2}{4 + 2\epsilon^2} y^2 \leq 0$$

holds true. In fact, we can obtain equality by letting $\epsilon = 1/\sqrt{2k}$, and the lemma is proved.

To conclude the proof of Theorem 3.2, use the result of Lemma 3.1 in equation (12) to obtain

$$\frac{\partial}{\partial t}(\frac{1}{2}\int_0^1 v^2(t,x)dx) \leq -\frac{1}{4 + 2\epsilon^2}\int_0^1 v^2(t,x)dx$$

with $\epsilon = 1/\sqrt{2k}$. Letting $\phi(t) = \frac{1}{2}\int_0^1 v^2(t,x)dx$, we have $\phi'(t) \leq -\frac{1}{2+\epsilon^2}\phi(t)$. Solving this by manipulation and integrating from $t = 0$ to $t = T$ to find

$$\phi(T) \leq \phi(0)e^{-T/(2+\epsilon^2)} = \phi(0)e^{-2kT/(4k+1)}.$$

Of course now we have

$$\int_0^1 (u(t,x) - c)^2 dx \leq Ce^{-2kt/(4k+1)}$$

where $C = \int_0^1 v^2(0,x)dx$ is a computable quantity. The theorem has been proven.

Theorem 3.2 will allow for the future simplification of calculations by assuming zero initial conditions and will also be helpful in calculating the error in our reconstruction for the function F.

4 Complete Data for $t > 0$: Characterizing the Defect

Let use assume that $u(t,x)$ satisfies equations (1)-(5) but with $f(x) = 0$. Let us also assume that we have noiseless measurements of the endpoint temperatures at all times $t > 0$, say

$$\begin{aligned} u(t,0) &= a(t) \\ u(t,1) &= b(t) \end{aligned}$$

for some known functions $a(t)$ and $b(t)$. Under these conditions we show that the location of the defect can be uniquely determined.

From equations (2) and (3), we are given the heat fluxes at $x = 0$ and $x = 1$. In fact, we can choose these fluxes. In an attempt to be as general as possible, we will solve for the location of the defect for any boundary fluxes, as long as at least one is nonzero. Using the flux information and the endpoint temperature measurements given above, the location of σ will be recovered without knowledge of F.

Theorem 4.1 *Suppose the fluxes $g_0(t)$, $g_1(t)$ are not both identically zero. Then these fluxes and the data $a(t)$, $b(t)$ for $t > 0$ uniquely determine σ.*

Proof. To prove this, we employ the Laplace Transform, defined by

$$\mathcal{L}(h(t)) = H(s) = \int_0^\infty e^{-st} h(t) dt.$$

Then equations (1)-(5) with the zero initial conditions become

$$\begin{aligned} sU(s,x) - U_{xx}(s,x) &= 0 \text{ in } (0,\sigma) \cup (\sigma,1) \\ -U_x(s,0) &= G_0(s) \\ U_x(s,1) &= G_1(s) \\ U_x(s,\sigma) &= \mathcal{L}(F([u](t))) \end{aligned} \tag{13}$$

Equation (13) can be solved on both $(0,\sigma)$ and $(\sigma,1)$, respectively, using simple techniques in ordinary differential equations, to yield solutions of the form

$$U_L(s,x) = c_1 e^{\sqrt{s}x} + c_2 e^{-\sqrt{s}x} \tag{14}$$

$$U_R(s,x) = d_1 e^{\sqrt{s}x} + d_2 e^{-\sqrt{s}x} \tag{15}$$

where $U_L(s,x)$ denotes the Laplace transform of $u(t,x)$ with respect to t for $0 < x < \sigma$ and $U_R(s,x)$ the transform for $\sigma < x < 1$. In order to find these constants, the endpoint data measurements should be brought into the Laplace domain. Let $A(s)$ and $B(s)$ denote the Laplace transforms of $a(t)$ and $b(t)$.

The constants c_1 and c_2 in equation (14) can be found for the $(0,\sigma)$ section of Ω by solving the system of equations formed by $U_x(s,0) = G_0(t)$ and $U(s,0) = A(t)$. A similar computation can be used to find the constants d_1 and d_2 in equation (15). We find

$$\begin{aligned} U_L(s,x) &= \left(\frac{A(s)}{2} - \frac{G_0(s)}{2\sqrt{s}}\right) e^{\sqrt{s}x} + \left(\frac{A(s)}{2} + \frac{G_0(s)}{2\sqrt{s}}\right) e^{-\sqrt{s}x} \\ U_R(s,x) &= \left(\frac{B(s)}{2} + \frac{G_1(s)}{2\sqrt{s}}\right) e^{\sqrt{s}(x-1)} + \left(\frac{B(s)}{2} - \frac{G_1(s)}{2\sqrt{s}}\right) e^{-\sqrt{s}(x-1)} \end{aligned} \tag{16}$$

Since $u_x(t,x)$ is continuous across $x = \sigma$ for all time (or in this case, for all s), we set $U_{L,x}(s,\sigma) = U_{R,x}(s,\sigma)$. Using two hyperbolic trigonometric identities

$$2\sinh(z) = e^z - e^{-z}$$
$$2\cosh(z) = e^z + e^{-z}$$

and a simple rearrangement, we get the following equation:

$$A(s)\sinh(\sqrt{s}\sigma) - \frac{G_0(s)}{\sqrt{s}}\cosh(\sqrt{s}\sigma) = B(s)\sinh(\sqrt{s}(\sigma-1)) + \frac{G_1(s)}{\sqrt{s}}\cosh(\sqrt{s}(\sigma-1)). \tag{17}$$

Applying the hyperbolic difference of angles formulas

$$\begin{aligned} \sinh(x-y) &= \sinh(x)\cosh(y) - \cosh(x)\sinh(y) \\ \cosh(x-y) &= \cosh(x)\cosh(y) - \sinh(x)\sinh(y) \end{aligned}$$

and collecting like terms, we can solve for σ uniquely:

$$\sigma = \frac{1}{\sqrt{s}}\tanh^{-1}\left(\frac{G_0(s) - B(s)\sqrt{s}\sinh(\sqrt{s}) + G_1(s)\cosh(\sqrt{s})}{A(s)\sqrt{s} - B(s)\sqrt{s}\cosh(\sqrt{s}) + G_1(s)\sinh(\sqrt{s})}\right). \tag{18}$$

Not only is σ determined by the boundary fluxes and endpoint temperature measurements, it is actually overdetermined. Any nonzero value of s except for those that give rise to singularities in

$G_0(s), G_1(s), A(s)$, and $B(s)$ or cause the denominator in (18) to vanish will yield the correct value for σ.

We now show that the denominator on the right in equation (18) cannot vanish for all s unless $u_x(t,\sigma) \equiv 0$. We proceed by contradiction. Suppose the denominator vanishes identically in s. This implies $A(s) = B(s)\cosh(\sqrt{s}) - \frac{G_1(s)}{\sqrt{s}}\sinh(\sqrt{s})$. Plugging this value into equation (17), we find that then $G_0(s) = B(s)\sqrt{s}\sinh(\sqrt{s}) - G_1(s)\cosh(\sqrt{s})$. These two equalities, when put into equation (16), show that $U_L(s,x) = U_R(s,x)$, and hence $u^-(t,\sigma) \equiv u^+(t,\sigma)$, i.e., $[u](t) \equiv 0$. From the properties of F we conclude that $u_x(t,\sigma) \equiv 0$. In short, if $u_x(t,\sigma)$ is NOT identically zero, equation (18) must yield the correct value for σ whenever the denominator is non-zero.

However, it is possible for the denominator to vanish identically, and so equation (18) fails to yield an estimate of σ (e.g., if $\sigma = 1/2$ and $g_0(t) \equiv g_1(t)$—from symmetry we obtain $u_x(t,1/2) \equiv 0$). Nonetheless, even in this case the defect location is still uniquely determined by the flux and temperature data.

To see this, consider solutions $u_1(t,x)$ and $u_2(t,x)$ to equations (1)-(5), with defect locations σ_1 and σ_2, respectively. Assume that $\frac{\partial u_1}{\partial x}(t,\sigma_1) \equiv 0$ and $\frac{\partial u_2}{\partial x}(t,\sigma_2) \equiv 0$ (so equation (18) fails) and that u_1 and u_2 have the same Cauchy data ($u_1(t,0) \equiv u_2(t,0)$ and both with input fluxes $g_0(t), g_1(t)$). We will show that $\sigma_1 = \sigma_2$.

Suppose, to the contrary, that $\sigma_1 \neq \sigma_2$, say $\sigma_1 < \sigma_2$. Since u_1 and u_2 have the same Cauchy data at $x = 0$ we must conclude from Theorem 3.1 that $u_1(t,x) \equiv u_2(t,x)$ for $0 \leq x \leq \sigma_1$. This implies that $\frac{\partial u_2}{\partial x}(t,\sigma_1) = \frac{\partial u_1}{\partial x}(t,\sigma_1) = 0$ for $t > 0$. Since $\frac{\partial u_2}{\partial x}(t,\sigma_2) \equiv 0$ and u_2 satisfies the heat equation for $\sigma_1 < x < \sigma_2$, we conclude that $u_2(t,x) \equiv 0$ for $\sigma_1 < x < \sigma_2$ and $t > 0$. This immediately implies that $u_2(t,x) \equiv 0$ for $0 \leq x \leq \sigma_2$ (by Theorem 3.1, since $u_2(t,\sigma_1) \equiv 0$). We are forced to conclude that $g_0(t) \equiv 0$. Similarly, since $\frac{\partial u_2}{\partial x}(t,\sigma_2) \equiv 0$ we have that $[u_2](t) \equiv 0$, forcing $u_2^+(t,\sigma_2) \equiv 0$. This, along with $\frac{\partial u_2}{\partial x}(t,\sigma_2) \equiv 0$, forces $u_2(t,x) \equiv 0$ for $\sigma_2 \leq x \leq 1$, and we conclude that $g_1(t) \equiv 0$ also, a contradiction.

This completes the proof of Theorem 4.1.

Note that although we have shown that any two distinct defects σ_1 and σ_2 must yield different endpoint data $a(t)$ and $b(t)$, we have not shown that any defect is "detectable". If $a(t)$ and $b(t)$ are the temperature measurements for a bar with defect at σ (input fluxes $g_0(t)$ and $g_1(t)$) and $a_0(t)$, $b_0(t)$ the data for a bar with no defect (same input fluxes). Then it IS possible that $a(t) \equiv a_0(t)$ and $b(t) \equiv b_0(t)$. Again, simply let $\sigma = 1/2$ with any F and $g_0(t) = g_1(t)$. Symmetry shows that the bar with defect at $\sigma = 1/2$ yields the same Cauchy data as the bar with no defect.

However, we can guarantee the "detectability" of any defect by taking, for example, $g_1(t) \equiv 0$ and any non-zero choice for $g_0(t)$. In this case the flux $u_x(t,\sigma)$ cannot vanish identically, for if so we would conclude that $u(t,x) \equiv 0$ for $\sigma < x < 1$, and hence on the entire bar, leading to the contradiction $g_0(t) \equiv 0$.

Since the identification of the defect's location has been accomplished, the focus now shifts to describing its influence on the heat flow, that is, the recovery of the function F. To do so, the problem will be converted back into the time domain.

Theorem 4.2 *The function F is uniquely determined (on the set of temperature jumps that occur) by the boundary fluxes $g_0(t)$ and $g_1(t)$, and the resulting temperature measurements at the endpoints, $a(t)$ and $b(t)$.*

Proof. Since the Laplace transform is injective, given $H(s)$, one can in principle determine $h(t)$. Thus, $U_L(s,x)$ and $U_R(s,x)$ have inverse Laplace transforms, which correspond to $u_L(t,x)$ and $u_R(t,x)$. The temperature jump at σ is defined as $[u](t) = u_R(t,\sigma) - u_L(t,\sigma)$ and the temperature flux at σ is defined as $u_{L,x}(t,\sigma) = u_{R,x}(t,\sigma)$. We can thus recover $[u](t)$ and $u_x(t,\sigma)$ for all $t > 0$, and hence we can recover $F(z)$ where z spans the range of temperature jumps which occur for $t > 0$.

This completes the proof of Theorem 4.2.

5 The Finite Time Data Version: Finding σ

So far the continuous data version, where the endpoint temperature measurements are known for all time, has been presented. This however is not practical for obvious reasons concerning the limitations and expenses of gathering temperature measurements. In sections 5-7, we are going to present the alternative, the finite-time data version of the problem, where the endpoint measurement data is sampled for the time period $(0, T)$. For practical purposes, it will be assumed that there are enough sampling points to create a negligible error in computing integrals involving $a(t)$ and $b(t)$. We will choose our endpoint fluxes as $g_0(t) = \delta(t)$ and $g_1(t) = 0$, where $\delta(t)$ is the Dirac delta function.

In this section, we compute the error in σ by making approximations for $A(s)$ and $B(s)$. From equation (18), the only error in σ introduced in the finite data version is from $A(s)$ and $B(s)$; everything else can be calculated exactly. The endpoint temperature measurements are only known for a limited time period $(0, T)$, so to approximate the Laplace transform of $a(t)$ (similarly for $b(t)$) we use

$$A(s) = \int_0^\infty a(t)e^{-st}dt \approx \int_0^T a(t)e^{-st}dt + \int_T^\infty a_\infty e^{-st}dt$$

where a_∞ is the constant value which $u(t, x)$ approaches as $t \to \infty$. We can easily compute, as in the proof of Theorem 3.2, that $a_\infty = \int_0^R (g_0(t) + g_1(t))\, dt$, where $g_0(t)$ and $g_1(t)$ are identically zero for $t > R$. The approximation is justified based on the reasoning that the Laplace transform will have two integral components—one that is exact for the time period $(0, T)$ and one which is an estimate. The estimate is reasonable since there is a known amount of energy put into the rod, and as t becomes large, this energy becomes evenly distributed in the rod (Theorem 3.2).

This approximation will create an error ϵ_a in $A(s)$ of the following form:

$$|\epsilon_a| = \left| \int_0^\infty a(t)e^{-st}dt - \left(\int_0^T a(t)e^{-st}\, dt + \int_T^\infty a_\infty e^{-st}\, dt \right) \right| = \left| \int_T^\infty (a(t) - a_\infty)e^{-st}\, dt \right|$$

Now we expect (but have not proved) that the quantity $|a(t)-a_\infty|$ can be bounded as $|a(t)-a_\infty| \leq Ce^{-\lambda(k)t}$ where $\lambda(k) > 0$. In this case we can bound

$$|\epsilon_a| \leq \frac{C}{s} e^{-\lambda(k)T} e^{-sT}.$$

A similar error bound ϵ_b can be computed for the $B(s)$ approximation.

To find the optimal s to calculate σ (the s value providing the most accurate defect location), consider the formula for σ to be a function of $A(s)$ and $B(s)$ (all other values are exact, as stated before). Thus, to minimize the error in σ, the following equation is considered:

$$\begin{aligned} \Delta\sigma &= \frac{\partial\sigma}{\partial A}\epsilon_a + \frac{\partial\sigma}{\partial B}\epsilon_b. \\ &= \frac{-\epsilon_a + \epsilon_a B(s)\sqrt{s}\sinh(\sqrt{s}) - \epsilon_b\sqrt{s}\sinh(\sqrt{s})A(s) + \epsilon_b\cosh(\sqrt{s})}{sA^2(s) - 2sA(s)B(s)\cosh(\sqrt{s}) - 1 + 2B\sqrt{s}\sinh(\sqrt{s}) + B^2(s)s}. \end{aligned}$$

We should emphasize that this uses the assumption that $g_0(t) = \delta(t)$ and $g_1(t) \equiv 0$.

Plotting this equation and finding the value of s such that $\Delta\sigma$ is minimum yields the optimal s to use to determine σ in equation (18). Therefore, complications that arise from limited temperature measurements can be taken into quantifiable account when recovering the location of the defect.

6 The Flux Recovery

As stated previously, in order to recover F, it is necessary to know both $[u](t)$ and $u_x(t,\sigma)$. Let us make the point now that F is only recoverable for the range of jump sizes $[u](t)$ which occur during the measured time interval. For simplicity, in the remainder of the paper we will assume that $g_1(t) \equiv 0$.

From Theorem 4.2, it is possible to get the flux and jump recovery *if we are given endpoint temperature measurements for all time* by taking the inverse Laplace transform of various functions. Of course, this is impossible to do in practice. In order to get an accurate recovery of the flux and jump, Fourier series are implemented rather than inverse Laplace transforms since the error is easier to quantify.

To recover both $[u](t)$ and $u_x(t,\sigma)$, a Fourier series will be created to describe them. This will then facilitate a reasonable reconstruction of F itself, which is defined as $F([u](t)) = u_x(t,\sigma)$. The accuracy of the reconstructed F will depend on the error in the data measurements themselves and the error arising from limited data. We present an error analysis of these methods, assuming again that we have enough data to neglect integration error. This section deals solely with the flux recovery.

6.1 Recovery of $u_x(t,\sigma)$

To get a recovery for F in the manner stated before, a Fourier series is first created to describe the flux. We utilize the identity

$$\begin{aligned}\int_a^b v(0,x)u(T,x)dx + \int_0^T (v_x(T-t,b)u(t,b) - v_x(T-t,a)u(t,a))dt \\ = \int_0^T (v(T-t,t)u_x(t,b) - v(T-t,a)u_x(t,a))dt \end{aligned} \tag{19}$$

where u and v both satisfy the heat equation for $t > 0$, $a < x < b$, and u has zero initial conditions. This identity is easily derived through integration by parts and is included in the Appendix.

Recall that the value of σ has already been determined. To minimize error, choose (a,b) to be either $(0,\sigma)$ or $(\sigma,1)$, such that $b-a$ is minimum. Without loss of generalization, we assume $(a,b) = (0,\sigma)$.

Thus, equation (19) is transformed into, after some rearrangement

$$\begin{aligned}\int_0^T v(T-t,\sigma)u_x(t,\sigma)dt = &- \int_0^\sigma v(0,x)u(T,x)dx + \int_0^T v(T-t,0)g_0(t,0)dt \\ &- \int_0^T (v_x(T-t,\sigma)u(t,\sigma) - v_x(T-t,0)a(t))dt \end{aligned} \tag{20}$$

In order to create a Fourier cosine or sine series for $u_x(t,\sigma)$, we look for test functions $v(t,x)$ which have the following properties:

P1. $v_t - v_{xx} = 0$

P2. $v(T-t,\sigma)$ takes the form of a sine or cosine

P3. $v_x(T-t,\sigma) = 0$

These properties ensure that the only terms left in the equations are computable, known quantities (in other words, the term $\int_0^T (v_x(T-t,\sigma)u(t,\sigma)$, which is not known, drops out). Also, this ensures that the Fourier coefficients for $u_x(t,\sigma)$ are indeed recoverable.

Lemma 6.1 *The functions*

$$v_1(t,x) = \frac{1}{2}e^{-\omega(x-\sigma)}\cos(2\omega^2 t - \omega(x-\sigma)) + \frac{1}{2}e^{-\omega(\sigma-x)}\cos(2\omega^2 t - \omega(\sigma-x)) \tag{21}$$

$$v_2(t,x) = \frac{1}{2}e^{-\omega(x-\sigma)}\sin(2\omega^2 t - \omega(x-\sigma)) + \frac{1}{2}e^{-\omega(\sigma-x)}\sin(2\omega^2 t - \omega(\sigma-x)) \tag{22}$$

both satisfy P1-P3.

This is easily proven by substituting v_1 and v_2 for v and checking each property P1-P3.

We make the assumption that $a(t)$ and $b(t)$ have died down to a relatively constant (as per Theorem 3.2). Furthermore, we know that this constant can be computed (with our particular input fluxes). We consider the error made by this substitution later.

Putting the test functions v_1 and v_2 into equation (20), using u_∞ for the limiting value of $u(T,x)$, and using the trigonometric identity $\sin(z) - \cos(z) = \sqrt{2}\sin(z - \frac{\pi}{4})$ yields

$$\begin{aligned}
\int_0^T u_x(t,\sigma)\cos(2\omega^2(T-t))dt &= -\frac{1}{2}\int_0^T g_0(t)(e^{\omega\sigma}\cos(2\omega^2(T-t)+\omega\sigma) \\
&+ e^{-\sigma\omega}\cos(2\omega^2(T-t)-\omega\sigma))\,dt \\
&- \frac{\sqrt{2}\omega}{2}\int_0^T a(t)(e^{\omega\sigma}\sin(2\omega(T-t)+\omega\sigma-\frac{\pi}{4}) \\
&+ e^{-\omega\sigma}\sin(2\omega^2(T-t)-\omega\sigma-\frac{\pi}{4}))dt \\
&+ u_\infty\int_0^\sigma \cos(\omega(\sigma-x))\cosh(\omega(\sigma-x))dx
\end{aligned} \tag{23}$$

$$\begin{aligned}
\int_0^T u_x(t,\sigma)\sin(2\omega^2(T-t))dt &= -\frac{1}{2}\int_0^T g_0(t)(e^{\omega\sigma}\sin(2\omega^2(T-t)+\omega\sigma) \\
&+ e^{-\sigma\omega}\sin(2\omega^2(T-t)-\omega\sigma))\,dt \\
&- \frac{\sqrt{2}\omega}{2}\int_0^T a(t)(e^{-\omega\sigma}\sin(2\omega(T-t)+\omega\sigma-\frac{\pi}{4}) \\
&- e^{\omega\sigma}\sin(2\omega^2(T-t)-\omega\sigma-\frac{\pi}{4}))dt \\
&+ u_\infty\int_0^\sigma \sin(\omega(\sigma-x))\sinh(\omega(\sigma-x))dx
\end{aligned} \tag{24}$$

It is crucial to note that the right side of each of the above equations is computable. Call these $K_1(\omega)$ and $K_2(\omega)$. Expand the left hand sides of the equations to get the system of integral equations

$$\begin{aligned}
\cos(2\omega^2 T)I_1(\omega) + \sin(2\omega^2 T)I_2(\omega) &= K_1(\omega) \\
\sin(2\omega^2 T)I_1(\omega) - \cos(2\omega^2 T)I_2(\omega) &= K_2(\omega)
\end{aligned}$$

with $I_1(\omega) = \int_0^T u_x(t,\sigma)\cos(2\omega^2 t)dt$ and $I_2(\omega) = \int_0^T u_x(t,\sigma)\sin(2\omega^2 t)dt$. Solving this system of equations for $I_1(\omega)$ and $I_2(\omega)$ we get

$$\begin{aligned}
I_1(\omega) &= K_2(\omega)\sin(2\omega^2 T) + K_1(\omega)\cos(2\omega^2 T) \\
I_2(\omega) &= -K_2(\omega)\cos(2\omega^2 T) + K_1(\omega)\sin(2\omega^2 T)
\end{aligned}$$

To find the Fourier coefficients for $u_x(t,\sigma)$, set $\omega = \sqrt{\frac{k\pi}{2T}}$, and assume a Fourier expansion for $u_x(t,\sigma)$. In I_1, assume $u_x(t,\sigma) = \sum_{j=0}^{\infty} c_j\cos(\frac{j\pi t}{T})$.

Then

$$I_1(\sqrt{\frac{j\pi}{2T}}) = \int_0^T \sum_{j=0}^{\infty} c_j \cos(\frac{j\pi t}{T}) \cos(\frac{k\pi t}{T}) = \sum_{j=0}^{\infty} \int_0^T c_j \cos(\frac{j\pi t}{T}) \cos(\frac{k\pi t}{T}) dt$$

Noting the orthogonality of the cosine functions on $(0, T)$ in the last integral, the Fourier cosine coefficients are computed:

$$c_j = \begin{cases} \frac{I_1(0)}{T} & : \quad j = 0 \\ \frac{2I_1(\sqrt{\frac{j\pi}{2T}})}{T} & : \quad j \neq 0 \end{cases}$$

To reiterate, $u_x(t, \sigma) = \sum_{j=0}^{\infty} c_j \cos(\frac{j\pi t}{T})$. Finding the Fourier sine coefficients is done in a similar fashion using I_2. Thus, we have found a Fourier sine and cosine reconstruction for $u_x(t, \sigma)$.

As stated before, these reconstructions are not exact. There are two sources of error in this analysis. First, we assumed in equation (20) that $u(T, x)$ is constant. But with limited data, with time only from $t = 0$ to $t = T$, there will be some discrepancy between $u(T, x)$ and u_∞, its limiting value in T. Second, error in the reconstruction will appear if the instrument measuring the endpoint temperature measurements has error (in other words, if there is some "noise" in $a(t)$ and $b(t)$). Both of these errors will be addressed separately in subsections 6.2 and 6.3.

6.2 Error from Limited Data

In this section we derive a simple error bound on c_j, the Fourier cosine coefficients, due to the truncation of the data at time T. Although the bound is far from sharp, it does illustrate that as T gets larger we can expect the estimate of c_j go become more accurate.

In equation (20), we replace $\int_0^\sigma v(0, x)u(T, x)dx$ with the approximation $u_\infty \int_0^\sigma v(0, x)dx$ giving an error of

$$\left| \int_0^\sigma (u(T, x) - u_\infty) v(0, x) dx \right|.$$

Applying Hölder's Inequality to this error yields

$$\begin{aligned} |\text{Error in } K_1, K_2| &= \left| \int_0^\sigma (u(T, x) - u_\infty) v(0, x) dx \right| \\ &\leq \left(\int_0^\sigma (u(T, x) - u_\infty)^2) dx \right)^{1/2} \left(\int_0^\sigma v^2(0, x) dx \right)^{1/2} \\ &\leq \left(\int_0^1 (u(T, x) - u_\infty)^2) dx \right)^{1/2} \left(\int_0^\sigma v^2(0, x) dx \right)^{1/2} \\ &\leq Ce^{\frac{-2kT}{4k+1}} \left(\int_0^\sigma v^2(0, x) dx \right)^{1/2} \end{aligned}$$

where C is a constant and the last inequality is derived from Theorem 3.2.

Using the test functions v_1 and v_2 defined in equations (21) and (22), and taking the "worst case" for the integral (making it as large as possible), we get

$$|\text{Error in } K_1(\omega),\, K_2(\omega)| \leq Ce^{\frac{-2kT}{4k+1}} \sqrt{\frac{1}{32\omega}(6 + 8\omega\sigma + 4e^{2\omega\sigma})}.$$

From this, the maximum error bounds in $K_1(\omega)$ and $K_2(\omega)$ are found to be the above values, which gives the maximum error bound in $I_1(\omega)$ (a similar computation for $I_2(\omega)$ can be made) to

be

$$|\text{Error in } I_1(\omega)| \leq Ce^{\frac{-2kT}{4k+1}}\sqrt{\frac{1}{32\omega}(6+8\omega\sigma+4e^{2\omega\sigma})}.$$

With $\omega = \sqrt{\frac{j\pi}{2T}}$, this error becomes

$$|\text{Error in } I_1(\sqrt{\tfrac{j\pi}{2T}})| \leq Ce^{\frac{-2kT}{4k+1}}\sqrt{\frac{\sqrt{2T}}{32\sqrt{j\pi}}(6+8\sigma\sqrt{\frac{j\pi}{2T}}+4e^{2\sqrt{\frac{j\pi}{2T}}\sigma})}.$$

Remembering that the Fourier coefficients are defined by $c_j = \frac{2I_1}{T}$ for $j \neq 0$, we find

$$\begin{aligned} |\text{Error in } c_j| &\leq \frac{2}{T}Ce^{\frac{-2kT}{4k+1}}\sqrt{\frac{\sqrt{2T}}{32\sqrt{j\pi}}(6+8\sigma\sqrt{\frac{j\pi}{2T}}+4e^{2\sqrt{\frac{j\pi}{2T}}\sigma})} \\ &\leq \frac{D\sqrt{\alpha+\beta\sqrt{j}+\gamma e^{\delta\sqrt{j}}}}{j^{1/4}} \end{aligned} \tag{25}$$

for $D, \alpha, \beta, \gamma, \delta$ are all constants. Note that as $T \to \infty$ the error in c_j (for any fixed j) approaches zero.

A simple calculation reveals that the error for c_0 is bounded by $\frac{Ce^{-\frac{2kT}{4k+1}}}{T}$

6.3 Error from Noise

The instruments used to measure the temperature at $x = 0$ and $x = 1$ are only accurate to a certain degree. Error in these measurements will affect the recovery of the flux and thus the later reconstruction of the function F. We will now compute the error in each Fourier coefficient that comes from this noise.

Let $a(t) = \tilde{a}(t) + \epsilon(t)$ be the temperature measurements at the $x = 0$, where $\tilde{a}(t)$ is the true temperature and $\epsilon(t)$ is the error in this measurement. The error this causes in $K_1(\omega)$ and $K_2(\omega)$ are respectively

$$\frac{\sqrt{2}\omega}{2}e^{\omega\sigma}\int_0^T \epsilon(t)\sin(2\omega^2(T-t)+\omega\sigma-\frac{\pi}{4})dt + \frac{\sqrt{2}\omega}{2}e^{-\omega\sigma}\int_0^T \epsilon(t)\sin(2\omega^2(T-t)-\omega\sigma-\frac{\pi}{4})dt$$
$$\frac{\sqrt{2}\omega}{2}e^{\omega\sigma}\int_0^T \epsilon(t)\cos(2\omega^2(T-t)+\omega\sigma-\frac{\pi}{4})dt + \frac{\sqrt{2}\omega}{2}e^{-\omega\sigma}\int_0^T \epsilon(t)\cos(2\omega^2(T-t)-\omega\sigma-\frac{\pi}{4})dt.$$

This can be seen from equations (23) and (24). We bound this error by bounding the integrals by the maximum value possible. Thus,

$$|\text{Error in } K_1(\omega),\, K_2(\omega)| \leq \frac{\sqrt{2}\omega}{2}e^{\omega\sigma}(T|\epsilon(t)|_\infty) + \frac{\sqrt{2}\omega}{2}e^{-\omega\sigma}(T|\epsilon(t)|_\infty) = \sqrt{2}\omega T|\epsilon(t)|_\infty\cosh(\omega\sigma)$$

where $|\epsilon(t)|_\infty$ is the maximum value of $|\epsilon(t)|$. This value can be computed in various ways. If, for example, the instrument measuring the endpoint temperature has an absolute maximum error, then that would be the value of $|\epsilon(t)|_\infty$. If the error in the reading is some percentage of the value of the temperature, then $|\epsilon(t)|_\infty$ will be the maximum temperature reading multiplied by this percentage.

The error in $I_1(\omega)$ (error in $I_2(\omega)$ can be computed similarly) after letting $\omega = \sqrt{\frac{j\pi}{2T}}$ is

$$|\text{Error in } I_1(\sqrt{\tfrac{j\pi}{2T}})| \leq \sqrt{j\pi T}|\epsilon(t)|_\infty\cosh(\sqrt{\frac{j\pi}{2T}}\sigma).$$

Again, since $c_j = \frac{2I_1}{T}$ for $j \neq 0$, we find

$$|\text{Error in } c_j| \leq 2\sqrt{\frac{j\pi}{T}}|\epsilon(t)|_\infty \cosh(\sqrt{\frac{j\pi}{2T}}\sigma). \tag{26}$$

Equation (26) illustrates that the difficulty of recovering the higher Fourier coefficients of $u_x(t,\sigma)$ increases exponentially with frequency j and with defect depth σ. We thus expect some kind of regularization to be required in the presence of any significant noise.

7 The Temperature Jump Recovery

A similar process is done to reconstruct $[u](t)$ as a Fourier series. The same two types of error, arising from limited data and noise in the data, will also be considered.

7.1 Recovery of $[u](t)$

Substituting $(a,b) = (0,\sigma)$ and $(a,b) = (\sigma,1)$ into equation (19), adding the resulting equations, inserting known values, and rearranging, yields

$$\begin{aligned}\int_0^T [u](t)v_x(T-t,\sigma)dt &= \int_0^\sigma v(0,x)u^-(T,x)dx + \int_\sigma^1 v(0,x)u^+(T,x)dx \\ &- \int_0^T (g_0(t)v(T-t,0))dt - \int_0^T (a(t)v_x(T-t,0) - b(t)v_x(T-t,1))dt\end{aligned}$$

where we have taken $g_1(t) \equiv 0$. As in the previous section, the substitution $u(T,x) = u_\infty$ is made. An error analysis to see how this substitution affects the resulting Fourier coefficients is presented in subsection 7.2.

The substitution transforms the above equation into

$$\begin{aligned}\int_0^T [u](t)v_x(T-t,\sigma)dt &= u_\infty \int_0^1 v(0,x)dx - \int_0^T (g_0(t)v(T-t,0))dt \\ &- \int_0^T (a(t)v_x(T-t,0) - b(t)v_x(T-t,1))dt\end{aligned} \tag{27}$$

As in the flux recovery, we must find test functions $v(t,x)$ which satisfy

P1. $v_t - v_{xx} = 0$

P2. $v_x(T-t,\sigma)$ takes the form of a sine or cosine.

These properties allow for the recovery of a Fourier series for $[u](t)$ since the right hand side of equation (27) can be computed exactly.

Lemma 7.1 *The functions*

$$v_1(t,x) = e^{-\omega x}\cos(2\omega^2 t - \omega x) \tag{28}$$

$$v_2(t,x) = e^{-\omega x}\sin(2\omega^2 t - \omega x) \tag{29}$$

both satisfy P1 and P2.

This is easily shown by substituting v_1 and v_2 for v and checking P1 and P2.

Put v_1 and v_2 into equation (27), denote the right sides by $K_1(\omega)$ and $K_2(\omega)$ respectively, and use the trigonometric identity $\sin(z) - \cos(z) = \sqrt{2}\sin(z - \frac{\pi}{4})$, to get

$$\sqrt{2}\omega e^{-\omega\sigma}\int_0^T [u](t)\sin(2\omega^2(T-t) - \omega\sigma - \frac{\pi}{4})dt = K_1(\omega) \tag{30}$$

$$-\sqrt{2}\omega e^{-\omega\sigma}\int_0^T [u](t)\sin(2\omega^2(T-t) - \omega\sigma + \frac{\pi}{4})dt = K_2(\omega) \tag{31}$$

We use simple trigonometric identities to get

$$\begin{aligned}\cos(\xi_1)I_1(\omega) - \sin(\xi_1)I_2(\omega) &= \frac{-K_1(\omega)e^{\omega\sigma}}{\omega\sqrt{2}} \\ \cos(\xi_2)I_1(\omega) - \sin(\xi_2)I_2(\omega) &= \frac{K_2(\omega)e\omega\sigma}{\omega\sqrt{2}}\end{aligned}$$

where $\xi_1 = 2\omega^2 T - \omega\sigma - \frac{\pi}{4}$, $\xi_2 = 2\omega^2 T - \omega\sigma + \frac{\pi}{4}$, $I_1(\omega) = \int_0^T [u](t)\sin(2\omega^2 t)dt$, and $I_2(\omega) = \int_0^T [u](t)\cos(2\omega^2 t)dt$. Solving this system of equations for $I_1(\omega)$ and $I_2(\omega)$,

$$\begin{aligned}I_1(\omega) &= -\frac{\sqrt{2}e^{\omega\sigma}}{2\omega}(\sin(\xi_1)K_2(\omega) + \sin(\xi_2)K_1(\omega)) \\ I_2(\omega) &= -\frac{\sqrt{2}e^{\omega\sigma}}{2\omega}(\cos(\xi_1)K_2(\omega) + \cos(\xi_2)K_1(\omega))\end{aligned}$$

Examining $I_1(\omega)$ with $\omega = \sqrt{\frac{j\pi}{2T}}$ and a Fourier sine representation for the jump $[u](t) = \sum_{j=1}^{\infty} c_j \sin(\frac{j\pi t}{T})$,

$$I_1(\sqrt{\frac{j\pi t}{T}}) = \int_0^T \sum_{j=1}^{\infty} c_k \sin(\frac{j\pi t}{T})\sin(\frac{k\pi t}{T})dt = \sum_{j=1}^{\infty}\int_0^T c_k \sin(\frac{j\pi t}{T})\sin(\frac{k\pi t}{T})dt$$

As in the flux reconstruction, the last integral contains orthogonal functions. Thus, the Fourier coefficients are

$$c_j = \frac{2I_1(\sqrt{\frac{j\pi}{2T}})}{T},$$

and a reconstruction for the jump is $[u](t) = \sum_{j=1}^{\infty} c_j \sin(\frac{j\pi t}{T})$.

7.2 Error from Limited Data

In equation (27) we replaced $\int_0^1 v(0,x)u(T,x)dx$ with the approximation $\int_0^1 v(0,x)dx$ giving an error of

$$\left|\int_0^1 (u(T,x) - u_\infty)v(0,x)dx\right|.$$

Applying Hölder's inequality, we get

$$\begin{aligned}|\text{Error in } K_1, K_2| &= \left|\int_0^1 (u(T,x) - u_\infty)v(0,x)dx\right| \\ &\leq \left(\int_0^1 (u(T,x) - u_\infty)^2 dx\right)^{1/2}\left(\int_0^1 v^2(0,x)dx\right)^{1/2} \\ &\leq Ce^{-\frac{2kT}{4k+1}}\left(\int_0^1 v^2(0,x)dx\right)^{1/2}\end{aligned}$$

where C is a constant and the second inequality is derived from Theorem 3.2.

Using the test functions v_1 and v_2 defined in equations (28) and (29), and taking the "worst case" for the integral (making it as large as possible), we get

$$|\text{Error in } K_1(\omega)| \leq Ce^{-\frac{2kT}{4k+1}}\sqrt{\frac{5}{8\omega}}$$

for v_1 and

$$|\text{Error in } K_2(\omega)| \leq Ce^{-\frac{2kT}{4k+1}}\sqrt{\frac{3}{8\omega}}$$

for v_2.

These equations give us a bound for the error made by the substitution. From this, the error in $I_1(\omega)$ (a similar computation for $I_2(\omega)$ can be made) is

$$\begin{aligned}|\text{Error in } I_1(\omega)| &\leq \frac{\sqrt{2}}{2}e^{\omega\sigma}(Ce^{-\frac{2kT}{4k+1}}\sqrt{\frac{3}{8\omega}}\sin(2\omega^2T-\omega\sigma-\frac{\pi}{4})+Ce^{-\frac{2kT}{4k+1}}\sqrt{\frac{5}{8\omega}}\sin(2\omega^2T-\omega\sigma-\frac{\pi}{4}))\\ &\leq \frac{\sqrt{2}}{2}e^{\omega\sigma}Ce^{-\frac{2kT}{4k+1}}\left(\frac{\sqrt{3}+\sqrt{5}}{\sqrt{8\omega}}\right).\end{aligned}$$

Letting $\omega=\sqrt{\frac{j\pi}{2T}}$, this error becomes

$$|\text{Error in } I_1(\sqrt{\tfrac{j\pi}{2T}})| \leq \frac{C(\sqrt{3}+\sqrt{5})}{2^{7/8}\pi^{1/4}}\frac{e^{\sqrt{\frac{j\pi}{2T}}\sigma-\frac{2kT}{4k+1}}T^{1/4}}{j^{1/4}}$$

Now remembering that $c_j=\frac{2I_1}{T}$, we have

$$\begin{aligned}|\text{Error in } c_j| &\leq \frac{C(\sqrt{3}+\sqrt{5})}{2^{3/4}\pi^{1/4}}\frac{e^{\sqrt{\frac{j\pi}{2T}}-\frac{2kT}{4k+1}}}{T^{3/4}j^{1/4}}\\ &\leq \frac{De^{\alpha\sqrt{j}-\beta}}{j^{1/4}} \qquad (32)\end{aligned}$$

for constants D,α,β.

7.3 Error from Noise

As in the flux recovery, the impact from the error in the instruments which gather the temperature measurements needs to be assessed. As before, let $a(t)=\tilde{a}(t)+\epsilon(t)$ be the temperature measurements at $x=0$, where $\tilde{a}(t)$ is the true temperature and $\epsilon(t)$ is the error in this measurement. The error this causes in $K_1(\omega)$ and $K_2(\omega)$ are respectively:

$$\begin{aligned}&\omega\int_0^T\epsilon(t)(\cos(2\omega^2(T-t))-\sin(2\omega^2(T-t)))\,dt,\\ &-\omega\int_0^T\epsilon(t)(\cos(2\omega^2(T-t))+\sin(2\omega^2(T-t)))\,dt\end{aligned}$$

Both integrals are easily bounded to yield

$$|\text{Error in } K_1(\omega),K_2(\omega)| \leq 2\omega|\epsilon(t)|_\infty$$

where $|\epsilon(t)|_\infty$ is the supremum of $\epsilon(t)$ on $(0,T)$. This yields an error bound on $I_1(\omega)$ (and a bound on $I_2(\omega)$ is similar) of

$$|\text{Error in } I_1(\omega)| \leq Ce^{\omega\sigma}|\epsilon(t)|_\infty$$

for some constant C. Since $c_j=\frac{2I_1}{T}$ and $\omega=\sqrt{\frac{j\pi}{2T}}$ we find an error bound of the form

$$|\text{Error in } c_j| \leq C|\epsilon(t)|_\infty e^{\sqrt{\frac{j\pi}{2T}}\sigma} \qquad (33)$$

for some constant C. As with the flux, we expect high frequencies (large j) to be difficult to recover, and the difficulty increases exponentially with defect depth σ.

8 Ill-Posedness and Examples

We have found bounds for various errors in the Fourier coefficients of the flux and jump reconstructions. All these bounds show the magnitude of error in c_j increases as j increases. So for sufficiently large j, c_j contains little information about the true Fourier coefficient; the coefficient has been greatly corrupted by noise. This is the *ill-posedness* of the inverse problem – certain high frequency detail information about the flux and jump are lost to noise. To mitigate this phenomenon, we cut off higher, more corrupted, modes of the Fourier expansion:

$$u_x(t,\sigma) \approx \sum_{j=0}^{N} c_j \cos(\frac{j\pi t}{T})$$

$$[u](t) \approx \sum_{j=1}^{N} c_j \sin(\frac{j\pi t}{T})$$

How does one pick an appropriate N? It is known that Fourier coefficients must die down to zero as j gets large. Error will instead force Fourier coefficients to increase in magnitude as j gets large (see, for example, equations (26) and (33)). So by inspection, one can pick an N where the Fourier coefficients appear to stop converging to zero. This is one method for reducing noise in the reconstruction. In addition, all the bounds we found show that for large T, error is reduced. This makes sense – the more data collected, the better the reconstruction.

To illustrate this, and show how a reconstruction is possible by this method, we gather four sets of simulated endpoint temperature data. The data were generated computationally, by reducing the problem (1)-(5) to a system of four integrals equations, then solving the integrals equations with a simple fixed-point iteration scheme (see [1]). The solutions are accurate to about 4 significant figures.

The first set has data collected for 1 second, the second for 2 seconds, the third for 3 seconds, and the fourth for 4 seconds. Each set of data was generated using

$$\begin{aligned} \sigma &= 0.25 \\ F(x) &= 0.8x + 3x^3 \\ g_0(t) &= \begin{cases} 4 & \text{for} \quad t \leq 0.25 \\ 0 & \text{for} \quad t > 0.25 \end{cases} \\ g_1(t) &= 0. \end{aligned}$$

We collected, for each set of data, 100 Fourier coefficients for both the flux and jump reconstructions.

Here are the results for the flux reconstruction using equations (23) and (24) to recover the Fourier expansion of $u_x(t,\sigma)$, for $T = 1$ and $T = 4$ seconds:

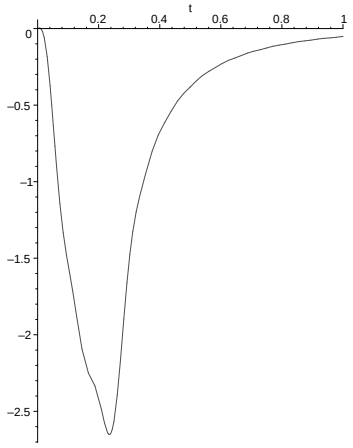

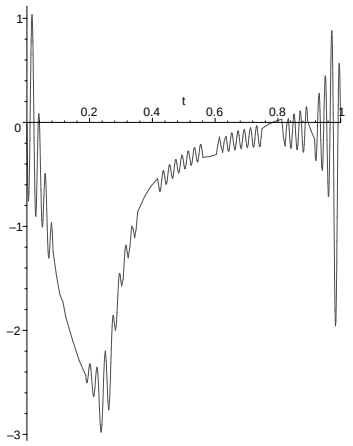

Flux Reconstruction: 4 Seconds Flux Reconstruction: 1 Second

Below are the reconstructions of $[u](t)$ using equations (30) and (31) to recover the Fourier expansion of $[u](t)$:

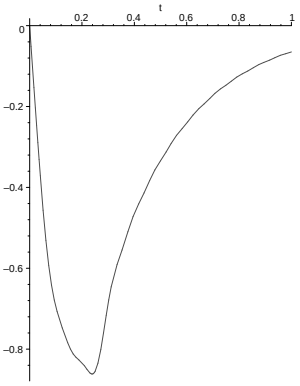

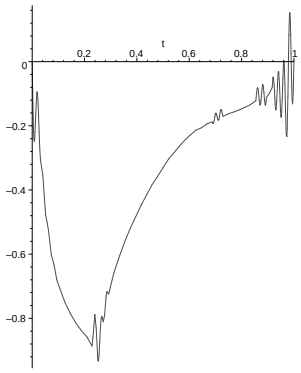

Jump Reconstruction: 4 Seconds Jump Reconstruction: 1 Second

Notice that in the figures above, the reconstruction made with less data (1 second) has a significantly more error in it.

We now include reconstructions of the function F, in order to demonstrate that a recovery is possible by these methods. Since $u_x(t,\sigma) = F([u](t))$, we show below a plot of $u_x(t,\sigma)$ versus $[u](t)$, which should approximate the graph of F.

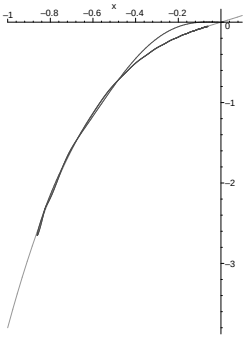

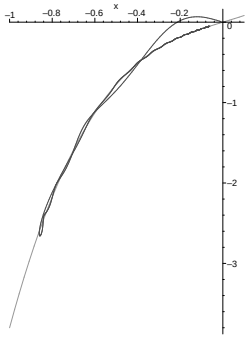

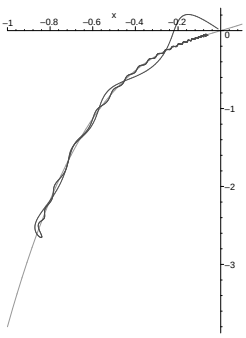

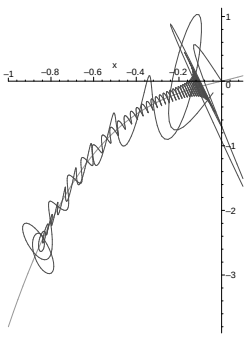

4 Seconds 3 Seconds 2 Seconds 1 Second

Of course, in the graphs above, the "shaky" lines are the reconstructions of F, and the smooth curve is the true graph of F. The more data there is, the closer the reconstruction is to the true value.

9 Conclusion

Our research in this paper shows that a description of a defect in the interior of a one-dimensional rod can be extracted from the response to a heat introduced at the boundaries. The use of domain transforms and Fourier series reconstructions provides an error-bounded means for using thermal imaging to find the location of the defect and compute its impact on heat flow. Our research can hopefully set precedence for future work in the use of thermal imaging for characterizing a defect in an object. Research involving multi-dimensional objects, multiple defects, and further variations on the boundary information are encouraged.

Appendix

We now present the derivation of Equation (19).

Consider the heat equation on some interval $a < x < b$, with $t > 0$ and zero initial conditions. Since $u_t - u_{xx} = 0$,

$$w(t,x)(u_t(t,x) - u_{xx}(t,x)) = 0$$

for any function $w(t,x)$. Integrating both sides of the equation from along the interval and for some length of time, and breaking the equation into two,

$$\int_a^b \int_0^T w(t,x)u_t(t,x) - \int_0^T \int_a^b w(t,x)u_{xx}(t,x)dxdt \quad = \quad 0 \tag{34}$$

Integrating the first piece above by parts in t to find

$$\int_a^b \int_0^T w(t,x)u_t(t,x)dtdx = \int_a^b w(T,x)u(T,x) - \int_a^b \int_0^T w_t(t,x)u(t,x)dtdx. \tag{35}$$

Now consider the second integral in (34). Integrate it by parts in x:

$$\int_0^T \int_a^b w(t,x)u_{xx}(t,x)dxdt = \int_0^T (w(t,b)u_x(t,b) - w(t,a)u_x(t,a))dt - \int_0^T \int_a^b w_x(t,x)u_x(t,x)dxdt.$$

Again, use integration by parts on the second integral above to obtain

$$\begin{aligned} \int_0^T \int_a^b w(t,x)u_{xx}(t,x)dxdt \quad = \quad & \int_0^T (w(t,b)u_x(t,b) - w(t,a)u_x(t,a))dt \\ & - \int_0^T (w_x(t,b)u(t,b) - w_x(t,a)u(t,b) - w_x(t,a)u(t,a))dt \\ & + \int_0^T \int_a^b w_{xx}(t,x)u(t,x)dxdt \end{aligned} \tag{36}$$

Using the right side of equation (35) to replace the first integral in (34), and the right side of equation (36) to replace the second integral in (34), and rearranging

$$\begin{aligned} & \int_0^T (w_x(t,b)u(t,b) - w_x(t,a)u(t,a))dt - \int_0^T (w(t,b)u_x(t,b) - w(t,a)u_x(t,a))dt \\ & - \int_0^T \int_a^b (w_t(t,x) + w_{xx}(t,x))u(t,x)dxdt + \int_a^b w(T,x)u(T,x)dx = 0 \end{aligned}$$

We now, to simplify this equation, put the constraint on w that it must satisfy the *backwards* heat equation $w_t + w_{xx} = 0$. It is easily checked that if $w(t,x) = v(T-t,x)$, then v satisfies the forward heat equation. From this we derive equation (19):

$$\int_a^b v(0,x)u(T,x)dx + \int_0^T (v_x(T-t,b)u(t,b) - v_x(T-t,a)u(t,a))dt$$
$$= \int_0^T (v(T-t,t)u_x(t,b) - v(T-t,a)u_x(t,a))dt$$

References

[1] Bryan, K. and Caudill, L. *Solvability of a Parabolic Boundary Value Problem with Internal Jump Condition*, Rose-Hulman Mathematics Technical Report MS 00-04, 2000.

[2] Cannon, J.R., "The One-Dimensional Heat Equation", Addison-Wesley, 1984.